SUPPLEMENTARY INFORMATION

Unless noted otherwise, all ageing experiments were performed on plates seeded with HT115(DE3) *E. coli* bacteria, carrying appropriate RNAi plasmid constructs (SEM: standard error of the mean; *P* values were calculated using the log-rank test, as described in Methods).

*Maximum lifespan shown is the median lifespan of the longest-lived 10% of the animals assayed.

†The number of confirmed death events, divided by the total number of animals included in lifespan assays is shown. Total equals the number of animals that died plus the number of animals that were censored (see Methods). The number of independent lifespan assays for each strain is shown in parentheses. The least number of animals followed for any strain tested was 127.

¶Assays were carried out at 25^{o}C.

#Compared with wild type animals subjected to control RNAi, assayed at the same temperature.

‡Compared with the corresponding mutant subjected to control RNAi.

**Assays were carried out at 15^{o}C.

§Animals were grown at 15^{o}C until the first day of adulthood, and subsequently transferred to 20^{o}C.

ns: no significant difference compared to control (P>0.05).

Supplementary Table 1. Lifespan data

Strain	Mean±SEM (days)	Max*±SEM (days)	Deaths /total†	*P* value
N2	20.4±1.08	26.3±1.03	586/777(5)	
N2; *phb-1(RNAi)*	17±0.3	22±0.5	435/740(5)	<0.0001#
N2; *phb-2(RNAi)*	18±0.4	23.2±0.7	398/734(5)	<0.0001#
daf-2(e1370)	40.5±1.5	57.4±4.2	257/399(2)	
daf-2(e1370); phb-1(RNAi)	61±0	93.9±2.8	349/422(2)	<0.0001‡
daf-2(e1370); phb-2(RNAi)	61+4	100.9±9	405/456(2)	<0.0001‡
daf-16(m26)	21.5±0.5	24.5±0.4	250/304(2)	
daf-16(m26); phb-1(RNAi)	18.5±3.5	22.6±4.4	250/357(2)	ns‡
daf-16(m26); phb-2(RNAi)	20±1	26.3±0.4	272/344(2)	ns‡
daf-16(m26); daf-2(e1370)	21±1	28.7±1.4	299/370(2)	
daf-16(m26); daf-2(e1370); phb-1(RNAi)	17±1	22.7±3.4	140/278(2)	<0.0001‡
daf-16(m26); daf-2(e1370); phb-2(RNAi)	20±2	30.4±2.2	376/455(2)	ns‡
daf-7(e1372)	23.2±1.9	32.8±1.2	213/289(4)	
daf-7(e1372); phb-1(RNAi)	33.7±2.5	51.8±3.5	390/606(4)	<0.0001‡
daf-7(e1372); phb-2(RNAi)	31.5±0.5	50.7±4.9	273.212(2)	<0.0001‡
*daf-4(m63)***	27±2	33.2±5.2	92/242(2)	
*daf-4(m63); phb-1(RNAi)***	41±0	50.7±0.1	228/301(2)	<0.0001‡
*daf-4(m63); phb-2(RNAi)***	44±1	53.8±0.9	254/301(2)	<0.0001‡
daf-11(m47)§	22±1	31.3±2.2	311/399 (2)	
daf-11(m47); phb-1(RNAi)§	27.5±0.5	45.8±6.2	274/379(2)	<0.0001‡
daf-11(m47); phb-2(RNAi)§	29.5±0.5	44.3±3.4	244/364(2)	<0.0001‡
eat-2(ad465)	21±1.5	29.2±2.7	223/421(3)	
eat-2(ad465); phb-1(RNAi)	27.6±0.3	47.2±3.2	410/494(3)	<0.0001‡
eat-2(ad465); phb-2(RNAi)	26.6±1.3	43.3±0.4	363/540(3)	<0.0001‡
clk-1(e2519)	18±1.2	30.2±2.1	404/584(4)	
clk-1(e2519); phb-1(RNAi)	29.7±0.2	41.3±2	557/672(4)	<0.0001‡
clk-1(e2519); phb-2(RNAi)	29.6±0.3	38.9±2	317/380 (3)	<0.0001‡
isp-1(qm150)	29.5±0.5	52.4±5.4	332/382(2)	
isp-1(qm150); phb-1(RNAi)	52.5±0.5	76.8±1.7	313/364(2)	<0.0001‡
isp-1(qm150); phb-2(RNAi)	45±1	66.2±0.2	264/303(2)	<0.0001‡
mev-1(kn1)	13.5±0.5	18.6±1.4	157/303(2)	
mev-1(kn1); phb-1(RNAi)	20.5±0.5	29±0.7	259/289(2)	<0.0001‡
mev-1(kn1); phb-2(RNAi)	20.5±0.5	30±1.2	237/288(2)	<0.0001‡
gas-1(fc21)	23.3±0.9	32.5±0.4	268/398(3)	
gas-1(fc21); phb-1(RNAi)	32±0.6	47.5±1.6	329/452(3)	<0.0001‡
gas-1(fc21); phb-2(RNAi)	32±0.6	43.4±3.4	229/411(3)	<0.0001‡
nhr-49(gk405)	14±1	16.9.5±1.1	212/318(2)	
nhr-49(gk405); phb-1(RNAi)	17.5±0.5	23.2±0.2	264/319(2)	<0.0001‡
nhr-49(gk405); phb-2(RNAi)	17.5±0.5	21.8±0.7	272/308(2)	<0.0001‡
fat-7(tm32/eT1)	17.5±1.5	23±0.9	247/337(2)	
fat-7(tm32/eT1); phb-1(RNAi)	25±1	39±2.8	262/337(2)	<0.0001‡
fat-7(tm32/eT1); phb-2(RNAi)	24±0	39.2±1.7	233/331(2)	<0.0001‡

Supplementary Table 1. *Continued.*

N2¶	13.6±0.4	20.6±0.96	605/720(5)	
N2; *phb-1(RNAi)*¶	17,2±0.37	22,9±0.74	505/623(5)	<0.0001#
N2; *phb-2(RNAi)*¶	17,4±0.75	23,4±1.3	599/747(5)	<0.0001#
geIn3	22,5±0,5	33,15±0,48	229/293 (2)	
geIn3; phb-1(RNAi)	23±2	34,09±1,73	212/289(2)	ns‡
geIn3; phb-2(RNAi)	20,5±1,5	35,92±0,92	310/370(2)	ns‡
sir-2.1(ok434)	19±0	24,45±2,55	215/273(2)	
sir-2.1(ok434); phb-1(RNAi)	19±0	26,32±0,81	253/299(2)	ns‡
sir-2.1(ok434); phb-2(RNAi)	19±0	26,38±0,88	217/271(2)	ns‡
gld-1(-)	13.5±0.96	15.9+0.9	321/430 (4)	
gld-1(-); phb-1(RNAi)	18±1.08	20.5±1.7	279/377(4)	<0.0001‡
gld-1(-); phb-2(RNAi)	17.25±0.85	21.6±1.7	314/383(4)	<0.0001‡
gld-1(+)	22.6±0.6	30.7+1.35	307/358 (3)	
gld-1(+); phb-1(RNAi)	23±1.5	33.4±1.47	336/375(3)	ns‡
gld-1(+); phb-2(RNAi)	23.6±2	29.8±2.9	229/372(3)	ns‡
daf-16(mu86)I; muEx151	14	20.6	41/59(1)	
daf-16(mu86)I; muEx151;phb-1(RNAi)	16	20.4	37/70(1)	ns‡
daf-16(mu86)I; muEx151;phb-2(RNAi)	14	21.3	39/72(1)	ns‡
daf-16(mu86)I; muEx116	17	23.2	89/108(1)	
daf-16(mu86)I; muEx116;phb-1(RNAi)	16	21	44/82(1)	0,0015
daf-16(mu86)I; muEx116;phb-2(RNAi)	16	21.2	82/105(1)	0,0004
mev-1(kn1) - NAC	16	22,3	76/98(1)	
mev-1(kn1); phb-1(RNAi) - NAC	20	34,1	85/100(1)	<0.0001‡
mev-1(kn1); phb-2(RNAi) - NAC	27	32,8	99/100(1)	<0.0001‡
mev-1(kn1) + NAC	20	25,6	86/155(1)	
mev-1(kn1); phb-1(RNAi) + NAC	27	35,3	85/108(1)	<0.0001‡
mev-1(kn1); phb-2(RNAi) + NAC	25	35,2	76/110(1)	<0.0001‡
N2 - NAC¶	13	21	76/98(1)	
N2; phb-1(RNAi) - NAC¶	17	23,1	85/100(1)	<0.0001‡
N2; phb-2(RNAi) - NAC¶	20	23,3	99/100(1)	<0.0001‡
N2 + NAC¶	15	17,7	70/125(1)	
N2; phb-1(RNAi) + NAC¶	17	24,1	64/98(1)	<0.0001‡
N2; phb-2(RNAi) + NAC¶	20	23,9	92/130(1)	<0.0001‡
N2 - NAC	20	28,6	90/100(1)	
N2; phb-1(RNAi) - NAC	17	27	99/141(1)	0,0835‡
N2; phb-2(RNAi) - NAC	17	26	120/151(1)	0,0778‡
N2 + NAC	17	27,3	64/80(1)	
N2; phb-1(RNAi) + NAC	17	24	56/112(1)	ns‡
N2; phb-2(RNAi) + NAC	17	22,3	34/85(1)	ns‡
aak-2(ok524)	22	28,1	146/150(1)	
aak-2(ok524); phb-1(RNAi)	20	25,7	130/151(1)	<0.0001‡
aak-2(ok524); phb-2(RNAi)	20	26,1	125/151(1)	<0.0001‡
cep-1(lg12501)	25±0	30.7±0.1	243/298 (2)	
cep-1(lg12501); phb-1(RNAi)	21.5±3.5	28.9±1	186/289(2)	<0.0001‡
cep-1(lg12501); phb-2(RNAi)	19±1	27.2±0.5	163/293(2)	<0.0001‡
lpIn1; jnk-1(+)	20	31,5	93/110(1)	
lpIn1; jnk-1(+); phb-1(RNAi)	20	31,5	105/146(1)	0.053‡
lpIn1; jnk-1(+); phb-2(RNAi)	23	31,8	94/150(1)	0.0008‡
jnk-1(gk7)	23	27,6	91/106(1)	
jnk-1(gk7); phb-1(RNAi)	16	23,9	77/106(1)	<0.0001‡
jnk-1(gk7); phb-2(RNAi)	16	22,6	93/110(1)	<0.0001‡
akt-1(ok525)	27	33,4	88/103(1)	
akt-1(ok525); phb-1(RNAi)	25	35,4	66/95(1)	ns‡
akt-1(ok525); phb-2(RNAi)	23	31,9	87/100(1)	0,0289‡
N2	19,3±0.66	24,9±0.78	250/286(3)	
N2; eat-3(RNAi)	24,3±0.66	32,7±0.46	233/282(3)	<0.0001‡
daf-2(e1370)	42±0	59,37±0.5	140/170(2)	
daf-2(e1370); eat-3(RNAi)	35,5±0.5	52,18±2.4	85/169(2)	0,0005‡

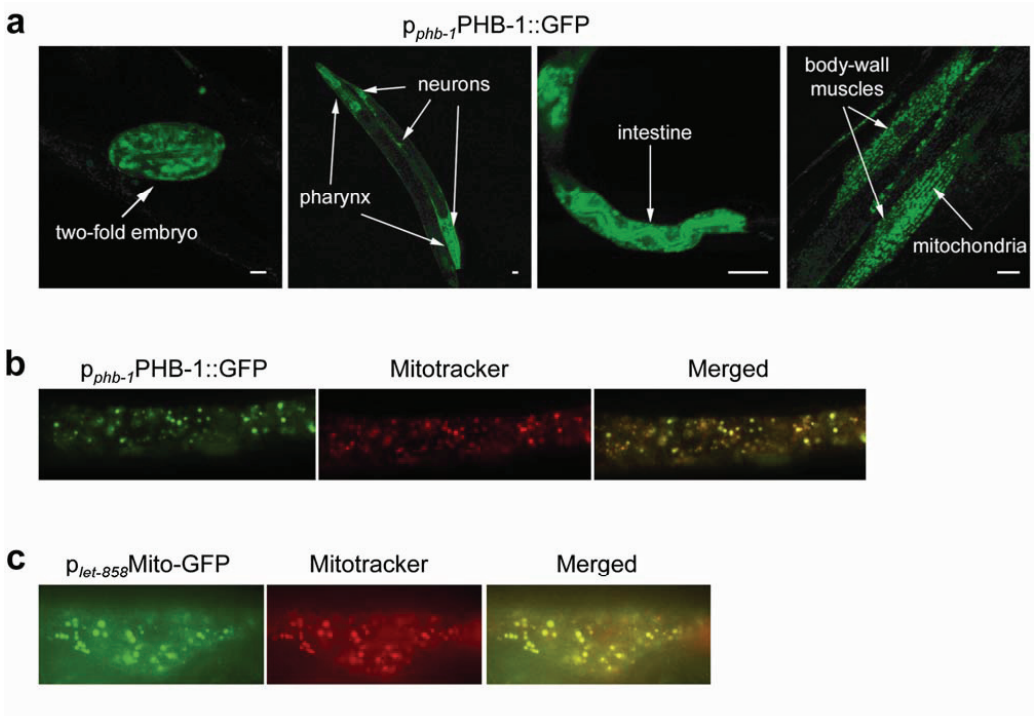

Figure S1 | **PHB-1 expression and subcellular localization. a,** Spatiotemporal expression and sub-cellular localization of prohibitin. Images of transgenic animals expressing a full-length p_{phb-1}PHB-1::GFP reporter fusion. *phb-1* is expressed in all somatic tissues of adult animals, including neurons, the pharynx, the intestine, body wall muscles (indicated by the arrows), the hypodermis, and the canal cell. Expression is detectable in two-fold stage embryos and remains high during all postembryonic developmental stages, throughout adulthood. Expression and sub-cellular localization of PHB-2 parallels that of PHB-1 (not shown). Both proteins co-localize in mitochondria (shown for muscle cells). White bars denote 10 microns. **b, c,** PHB-1::GFP co-localizes with mitochondria. Transgenic animal expressing a full-length p_{phb-1}PHB-1::GFP reporter fusion (b) or a $p_{let-858}$Mito-GFP reporter fusion (c), localizing in mitochondria. Animals were fed Mitotracker Deep Red 633 (Invitrogen, Molecular Probes).

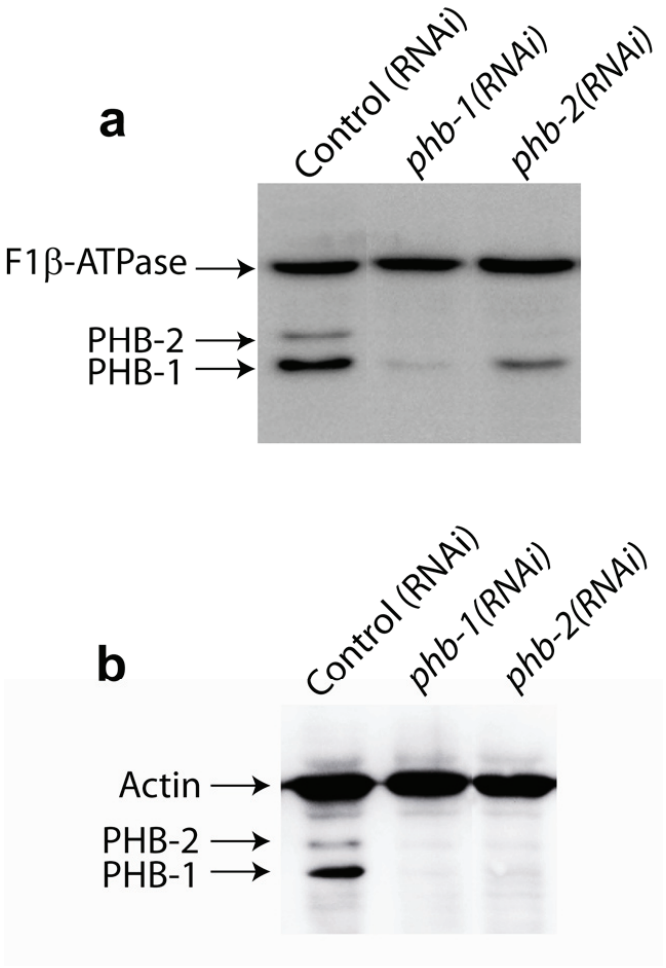

Figure S2 | **RNAi knockdown of *phb-1* and *phb-2* genes. a, b,** Western blot analysis of animals subjected to RNAi for both prohibitin genes. Two loading controls were used, F1β-ATPase (a) and actin (b), in two independent experiments. Bands corresponding to the two PHB proteins and the loading controls are indicated by arrows. RNAi with either *phb-1* or *phb-2* diminishes the levels of both PHB proteins perhaps by destabilizing the prohibiting complex[1].

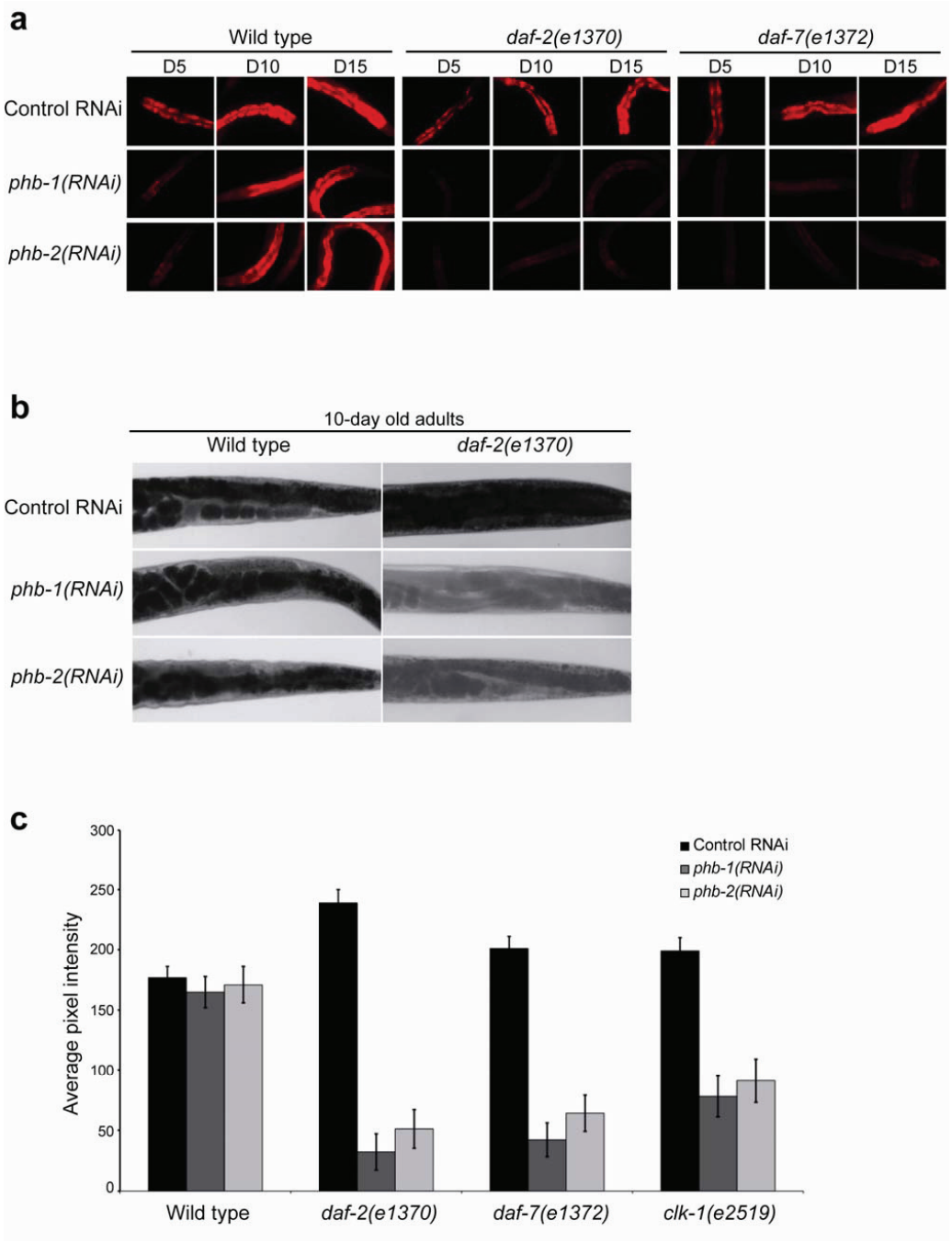

Figure S3 | **Fat staining by Nile red and Sudan black. a,** Nile red staining of intestinal lipid depositions in wild type animals and *daf-2* or *daf-7* mutants subjected to RNAi with either *phb-1* or *phb-2*. Images were acquired under the same exposure, using a 20x objective lens, at day 5, day 10 and day 15 of adulthood (D5, D10, and D15 respectively; see Methods; the anterior half of the animals is shown). **b,** Representative images of Sudan black-stained 10-day old wild type and *daf-2(e1370)* adults after depletion of PHB-1 and PHB-2. **c,** Quantification of Sudan black in wild type and *daf-2(e1370), daf-7(e1372)* and *clk-1(e2519)* mutants subjected to RNAi with either *phb-1* or *phb-2* (see Supplementary Methods; error bars denote standard deviation; $P<0.005$, unpaired *t* test; assays were carried out at 20°C).

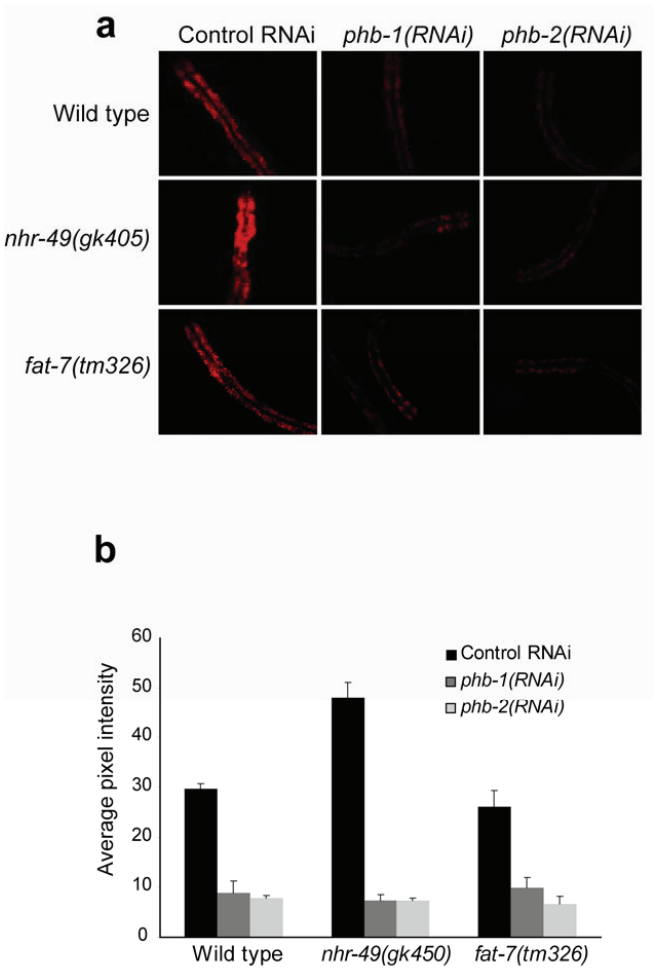

Figure S4 | **Nile red staining of mutants defective in fat metabolism. a,** Elimination of prohibitin diminishes intestinal fat content in both wild type and fat-metabolism-deficient mutants. In addition, lack of prohibitin fully suppresses the elevated intestinal lipid deposition phenotype of *nhr-49* mutant animals. Images were acquired on the second day of adulthood, under the same exposure with a 20x objective lens capturing the anterior half of the animal. **b,** Quantification of intestinal fluorescence after Nile red staining of wild type animals and fat metabolism-defective mutants, subjected to RNAi with either *phb-1* or *phb-2*, on the second day of adulthood (see Methods; error bars denote standard deviation; $P<0.005$, unpaired t test; assays were carried out at 20°C). Survival curves depict the percentage of animals remaining alive, plotted against animal age. Lifespan values are given in Supplementary Table 1; assays were carried out at 20°C.

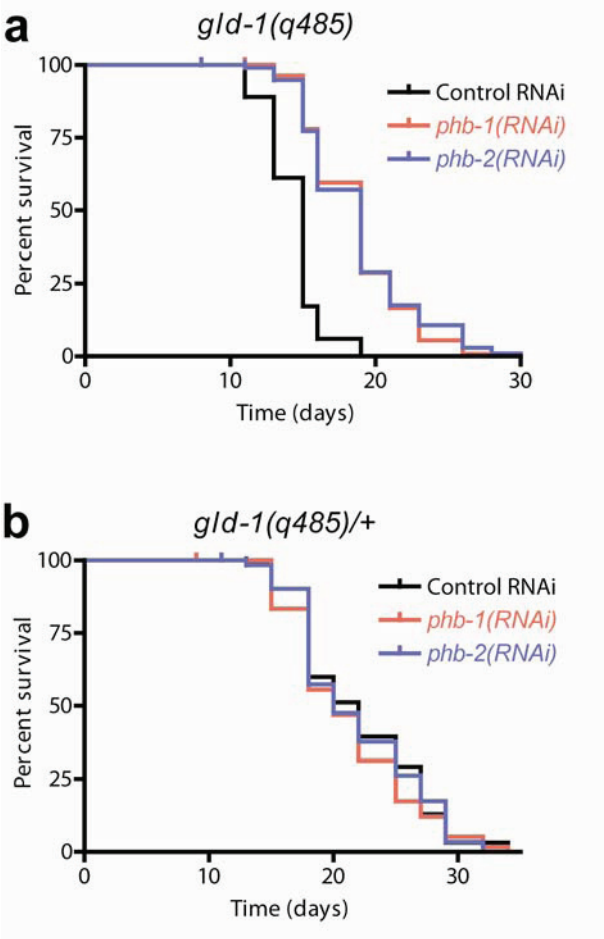

Figure S5 | **Prohibitin knockdown antagonizes germ cell overproliferation/germline tumour growth**. **a,** Depletion of prohibitin suppresses germline tumour formation (reduces germ-cell proliferation) and increases the lifespan of homozygous *gld-1(q485)* null mutants. **b,** Prohibitin knock-down does not affect the lifespan of heterozygous *gld-1(q485)/+* animals that do not suffer from germline tumours (germ-cells do not overproliferate). Survival curves depict the percentage of animals remaining alive, plotted against animal age. Lifespan values are given in Table 1; assays were carried out at 20°C.

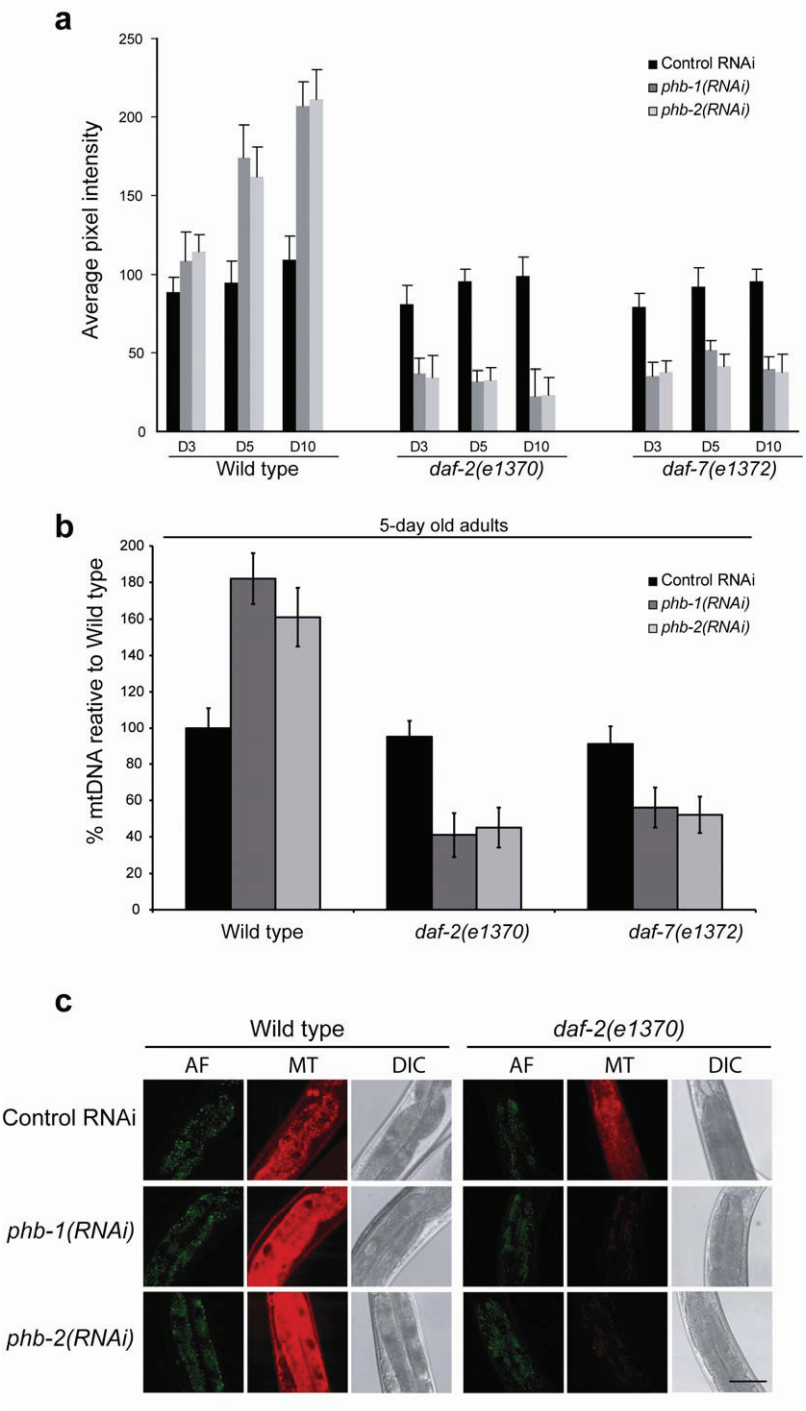

Figure S6 | **Analysis of Mitochondrial content. a,** Quantification of Mitotracker Deep Red 633 staining of intestinal mitochondria in wild type animals and dauer-defective *daf-2* or *daf-7* mutants subjected to RNAi with either *phb-1* or *phb-2*, at day 3, day 5 and day 10 of adulthood (D3, D5, and D10 respectively; see Methods; error bars denote standard deviation; $P<0.005$, unpaired *t* test; assays were carried out at 20°C). **b,** Mitochondrial DNA quantification. The percentage of mitochondrial DNA relative to wild type is shown. Quantitative PCR was performed at day 5 of adulthood in wild type, *daf-2(e1370)* and *daf-7(e1372)* mutant animals subjected to RNAi with either *phb-1* or *phb-2*. Error bars denote SEM; $P<0.005$, unpaired *t* test; assays were carried out at 20°C. **c,** Specificity of Mitotracker Deep Red 633. Images of wild type and *daf-2(e1370)* mutant animals after RNAi knock-down of either *phb-1* or *phb-2*. Left panel: intestinal auto-fluorescence (AF). Middle panel: Mitotracker staining (MT). Right panel: DIC images (differential interference contrast; Nomarski). Images were acquired on the fifth and tenth day of adulthood, under the same exposure with a 40x objective lens capturing the anterior part of the animal, the head is located at the top (bar: 50 μm).

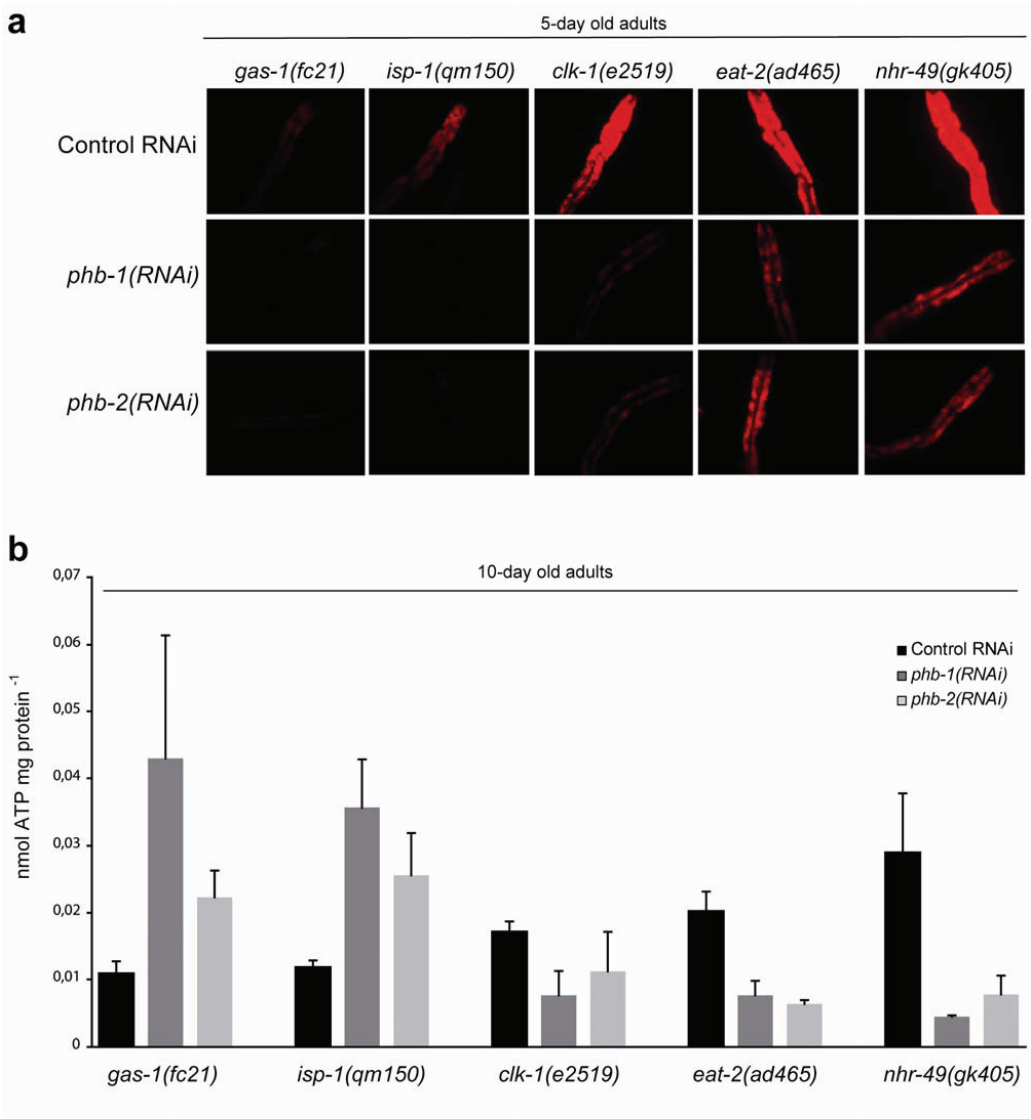

Figure S7 | **Effects of prohibitin depletion on energy metabolism. a,** Nile red staining of intestinal lipid depositions in different mutant genetic backgrounds subjected to RNAi with either *phb-1* or *phb-2*. Images were acquired under the same exposure, using a 20x objective lens at day 5 of adulthood. The anterior part of the intestine is shown. **b,** ATP levels after RNAi knock-down of either *phb-1* or *phb-2*. Prohibitin depletion increases ATP levels in the mitochondrial electron transport chain (ETC) mutants *gas-1(fc21)* and *isp-1(qm150)*, whereas it decreases ATP levels in *eat-2(ad465)* and *nhr-49(gk405)* mutants. Animals were measured at day 10 of adulthood (error bars denote standard deviation; $P<0.005$, unpaired *t* test; assays were carried out at 20°C).

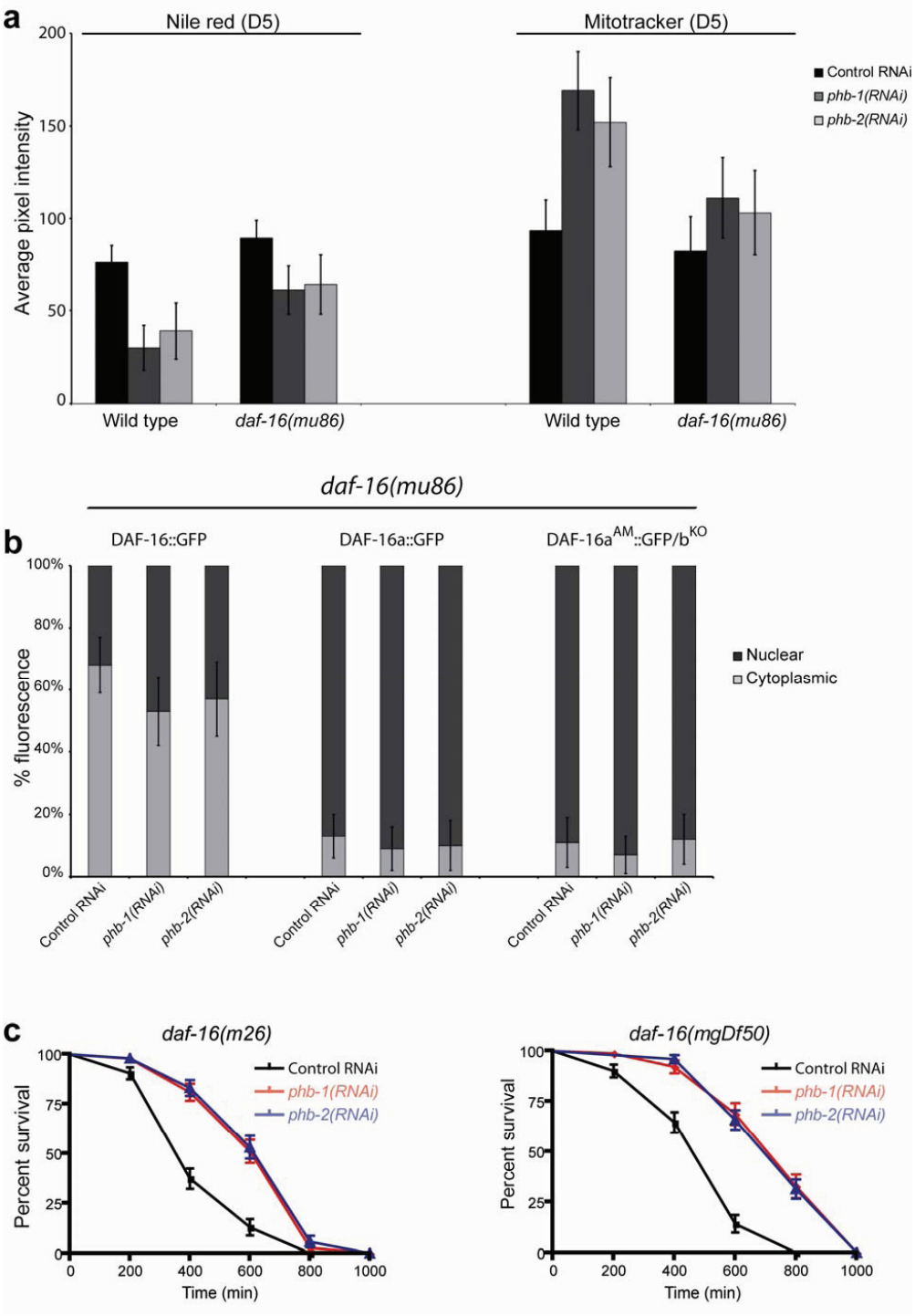

Figure S8 | Prohibitin and DAF-16. a, Quantification of Nile red (left) and Mitotracker (right) staining at day five of adulthood (D5), of wild type animals and *daf-16(mu86)* mutants, subjected to RNAi with either *phb-1* or *phb-2* (see Methods; error bars denote standard deviation; $P<0.005$, unpaired *t* test; assays were carried out at 20°C). **b,** Prohibitin depletion does not affect DAF-16 localisation. Percentage of nuclear and cytosolic DAF-16::GFP in different transgenic *daf-16(mu86)* mutant lines subjected to RNAi with either *phb-1* or *phb-2*. Depletion of prohibitins does not significantly affect the localisation of either wild-type DAF-16::GFP (left panel) or the localisation of two constitutively nuclear mutant forms of DAF-16[2] (DAF-16a^{AM}::GFP and DAF-16a^{AM} ::GFP/b^{KO}). Error bars denote standard deviation; $P<0.005$, unpaired *t* test; assays were carried out at 20°C. **c,** Thermotolerance of prohibitin depleted animals is DAF-16-independent. Thermotolerance of *daf-16* mutants subjected to RNAi with either *phb-1* or *phb-2*. Survival curves depict the percentage of animals remaining alive, plotted against time (minutes), at the elevated temperature (35°C). Error bars denote standard deviation.

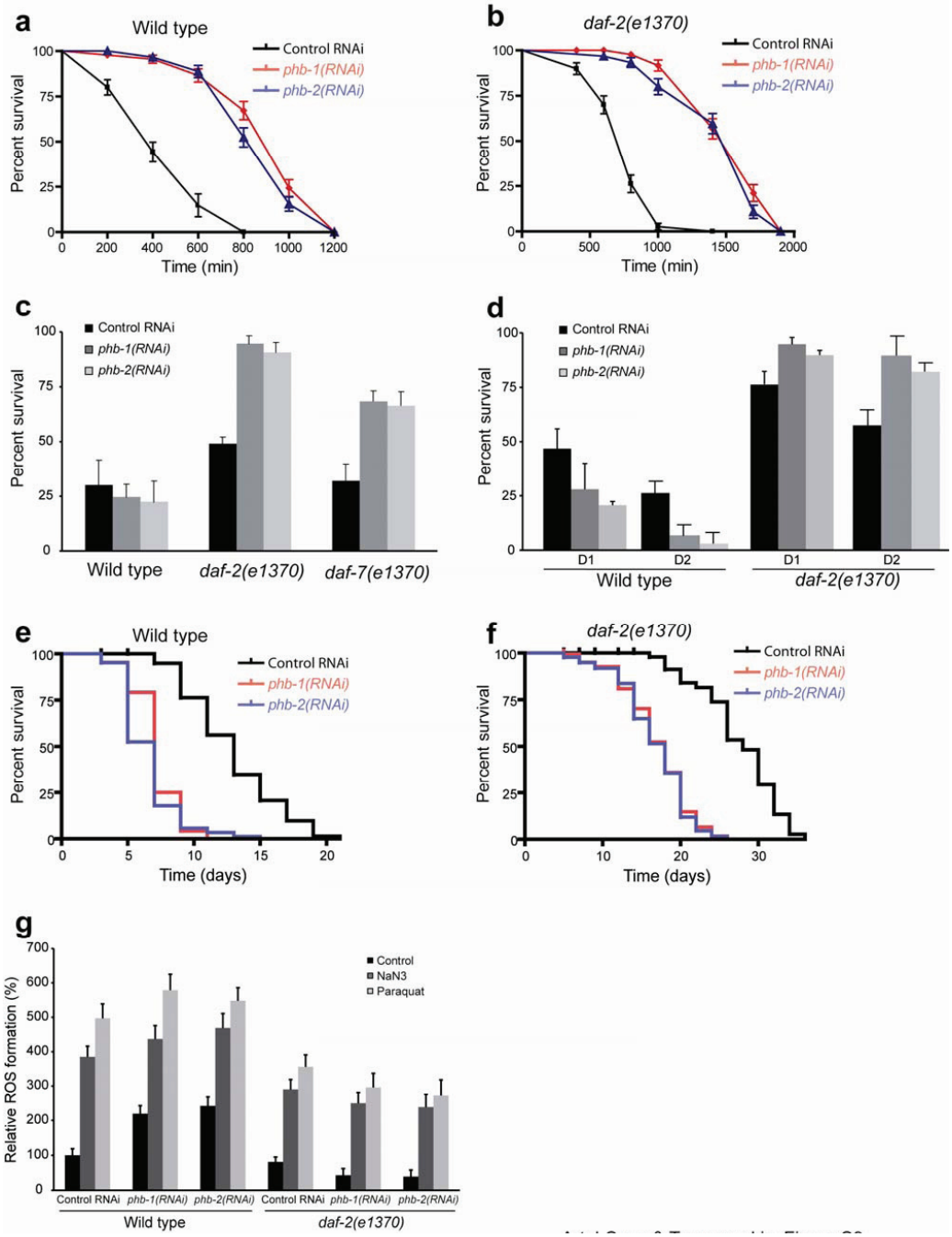

Figure S9 | **Effect of prohibitin depletion on stress resistance. a,** Thermotolerance of wild type animals versus animals subjected to RNAi with either *phb-1* or *phb-2*. **b,** Thermotolerance of *daf-2* diapause mutants subjected to RNAi with either *phb-1* or *phb-2*. Survival curves depict the percentage of animals remaining alive, plotted against time (minutes), at the elevated temperature (35°C). Error bars denote standard deviation. **c,** Survival of synchronized adult animal populations under oxidative stress induced by treatment with sodium azide. **d,** Survival of synchronized adult wild type and *daf-2* mutant animal populations subjected to *phb-1* or *phb-2* RNAi after treatment with paraquat at day 8 (day 1 of treatment; D1) and day 9 (day 2 of treatment; D2) of adulthood. Assays were carried out at 20°C, as described in the Methods section (three independent experiments, 300 animals total for each strain; error bars denote standard deviation; $P<0.005$, unpaired *t*-test). **e, f,** Survival of L4-stage wild type (e) and *daf-2* mutant (f) animal populations subjected to *phb-1* or *phb-2* RNAi after treatment with 2mM paraquat. Assays were carried out at 20°C. **g,** Measurement of ROS production in adult wild type and *daf-2* mutant animal populations subjected to *phb-1* or *phb-2* RNAi after treatment with sodium azide or paraquat.

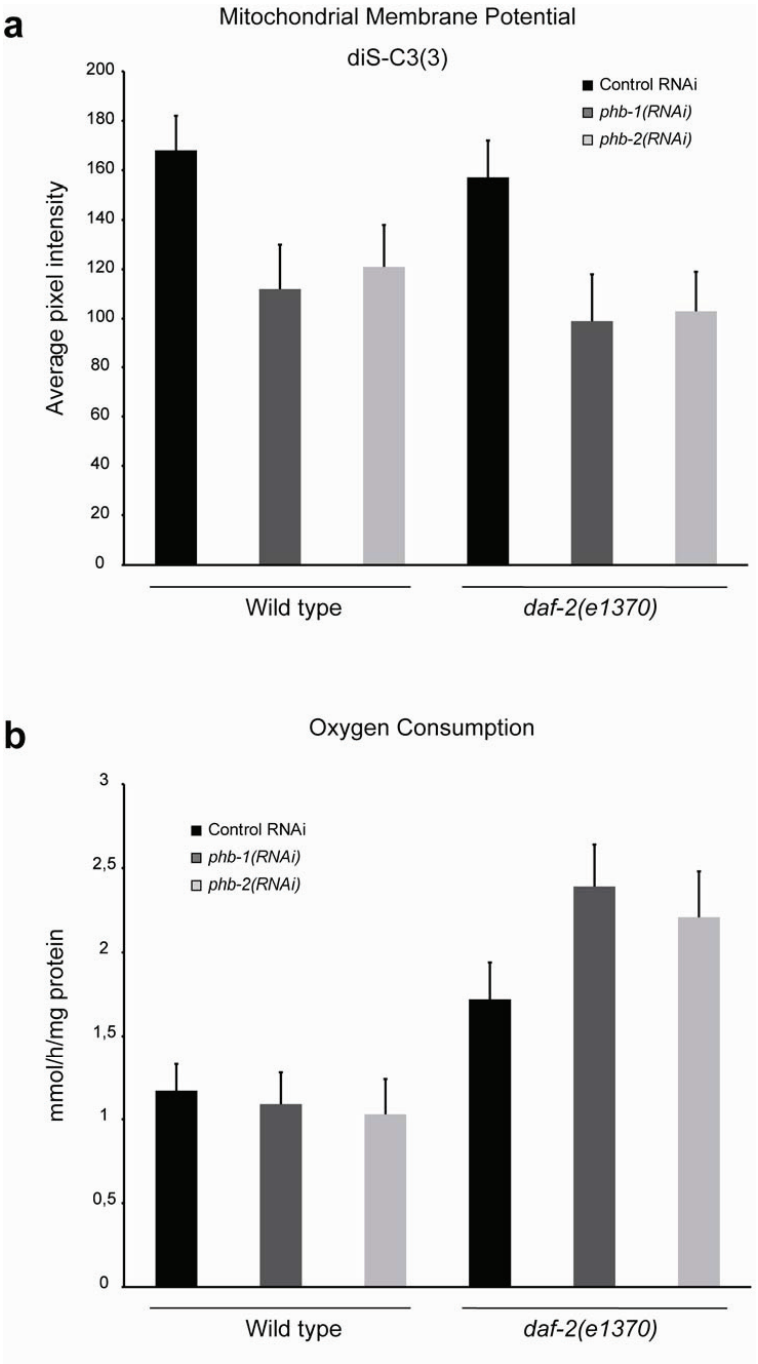

Figure S10 | Effect of *phb-1* and *phb-2* knockdown on mitochondrial membrane potential and oxygen consumption. a, Quantification of pharyngeal fluorescence after DiS-C(C3) staining of wild type animals and *daf-2(e1370)* mutants, subjected to RNAi with either *phb-1* or *phb-2* at day 5 of adulthood (see Supplementary Methods). RNAi for either *phb-1* or *phb-2* results in reduced mitochondrial membrane potential in both, wild type and *daf-2(e1370)* mutant animals **b,** Oxygen consumption rates of wild type and *daf-2(e1370)* mutants subjected to either *phb-1* or *phb-2* RNAi at day 5 of adulthood. Depletion of prohibitin does not significantly alter oxygen consumption of wild type animals, while it significantly increases oxygen consumption of *daf-2(e1370)* mutant animals. Error bars denote the standard error of the mean; $P<0.005$, unpaired *t* test; assays were carried out at 20°C).

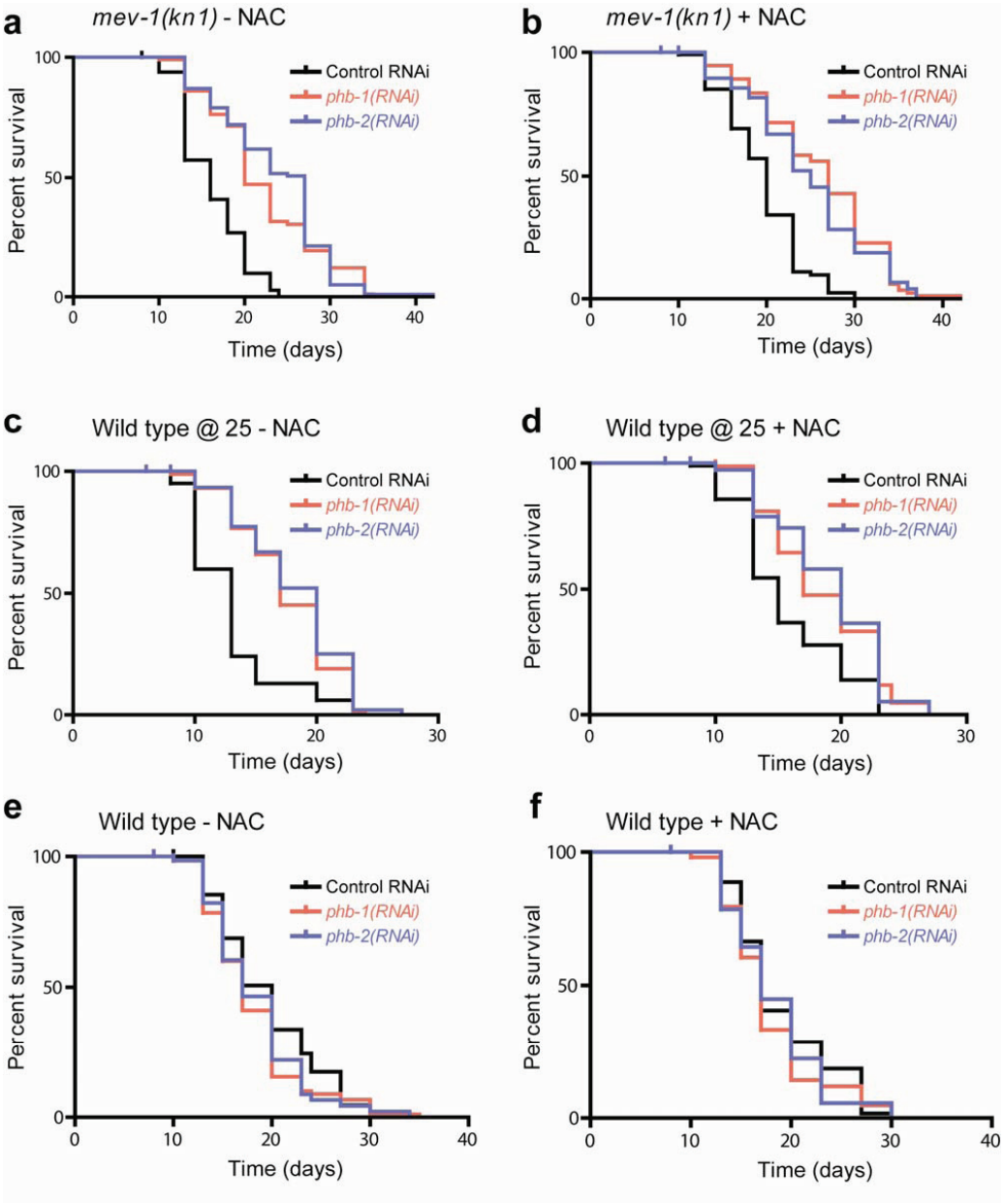

Figure S11 | The free-radical scavenger N-acetylcysteine (NAC) does not prevent the lifespan extension conferred by prohibitin depletion. Survival curves of *mev-1(kn1)* and wild type animals subjected to *phb-1* or *phb-2* RNAi in the presence or absence of NAC are shown. **a, b,** Knock-down of prohibitin in mutants carrying a lesion in the *mev-1* gene, a component of the mitochondrial electron transport chain complex II, in the absence and presence of NAC, respectively. **c, d,** Knock-down of prohibitin in wild type animals at 25°C in the absence and presence of NAC, respectively. **e, f,** Knock-down of prohibitin in wild type animals at 20°C in the absence and the presence of NAC, respectively. The percentage of animals remaining alive is plotted against animal age. Lifespan values are given in the Supplementary Table 1.

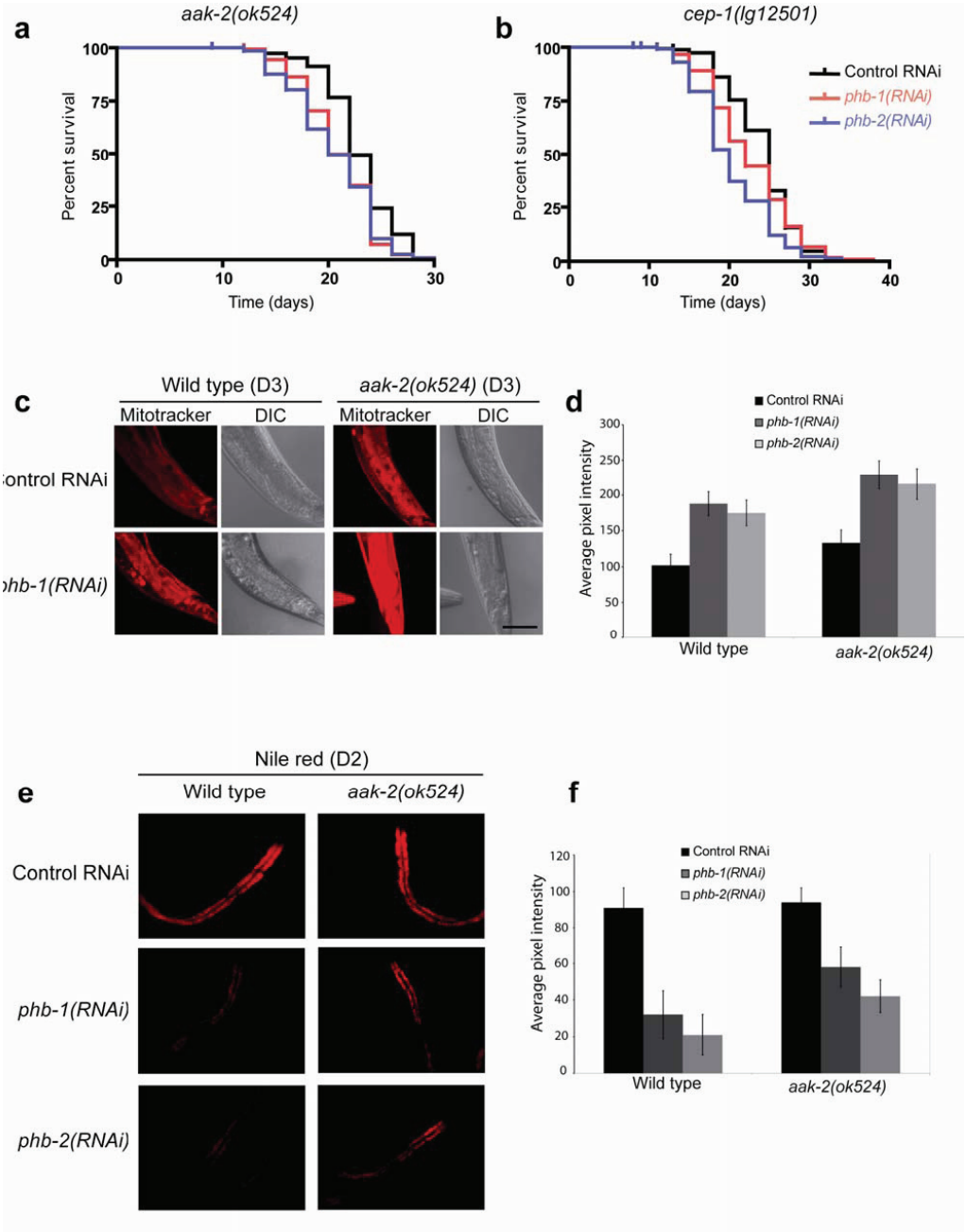

Figure S12 | Prohibitin and the AMPK-activated protein kinase pathway. a, b, Survival curves of *aak-2(ok534)* (AMPK) and *cep-1 (lg12510)* (p53) mutants, respectively, subjected to either *phb-1* or *phb-2* RNAi. The percentage of animals remaining alive is plotted against animal age. Lifespan values are given in the Supplementary Table 1. **c,** Mitotracker Deep Red 633 staining of intestinal mitochondria in wild type animals and *aak-2(ok524)* mutants subjected to *phb-1* RNAi. Images were acquired under the same exposure, using a 40x objective lens at day 3 (D3) of adulthood (the posterior part of the intestine is shown, the end of the tail is located to the bottom; bar: 50 μm) **d,** Quantification of Mitotracker intestinal fluorescence of wild type and *aak-2* mutants subjected to either *phb-1* or *phb-2* RNAi. Images were acquired under the same exposure, using a 40x objective lens. Animals were analysed at day 5 (D5) of adulthood (see Methods; error bars denote standard deviation; $P<0.005$, unpaired *t* test; assays were carried out at 20°C). **e,** Nile red staining of intestinal lipid depositions of wild type and *aak-2(ok524)* mutant animals after RNAi against either *phb-1* or *phb-2.* Images were taken under the same exposure at the second day of adulthood (D2). **f,** Quantification of intestinal fluorescence after Nile red staining of wild type and *aak-2* mutants (see Methods; error bars denote standard deviation; $P<0.005$, unpaired *t* test; assays were carried out at 20°C).

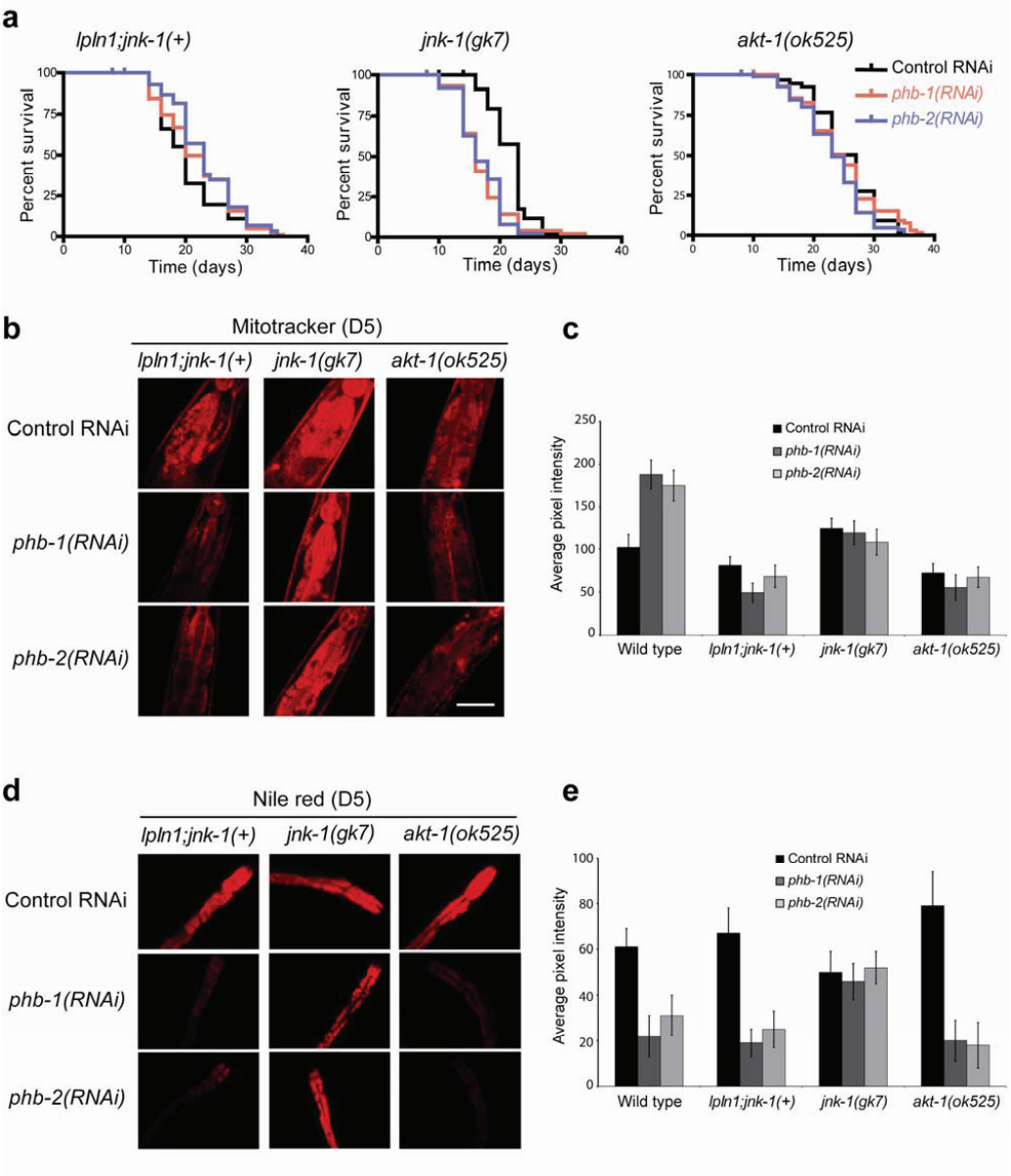

Figure S13 | **Prohibitin and the JNK-1 and AKT-1 kinase pathways**. **a,** Survival curves of transgenic animals overexpressing the c-Jun N-terminal kinase JNK-1, and *jnk-1(gk7)* or *akt-1(ok525)* mutant animals, subjected to either *phb-1* or *phb-2* RNAi. The percentage of animals remaining alive is plotted against animal age. Lifespan values are given in the Supplementary Table 1. **b,** Mitotracker Deep Red 633 staining of intestinal mitochondria of animals overexpressing or lacking JNK-1 and animals lacking AKT-1 after RNAi against either *phb-1* or *phb-2.* Images were acquired under the same exposure, using a 40x objective lens; bar: 50 µm. **c,** Quantification of Mitotracker intestinal fluorescence of wild type, overexpressing JNK-1 animals and *jnk-1* or *akt-1* mutants (see Methods; error bars denote standard deviation; $P<0.005$, unpaired *t* test; assays were carried out at 20°C). **d,** Nile red staining of intestinal lipid depositions in the strains mentioned above. Images were acquired under the same exposure, using a 20x objective lens. Animals were analysed at day 5 of adulthood. The anterior part of the intestine is shown. **e,** Quantification of intestinal fluorescence after Nile red staining of wild type, overexpressing JNK-1 animals and *jnk-1* and *akt-1* mutants (see Methods; error bars denote standard deviation; $P<0.005$, unpaired *t* test; assays were carried out at 20°C).

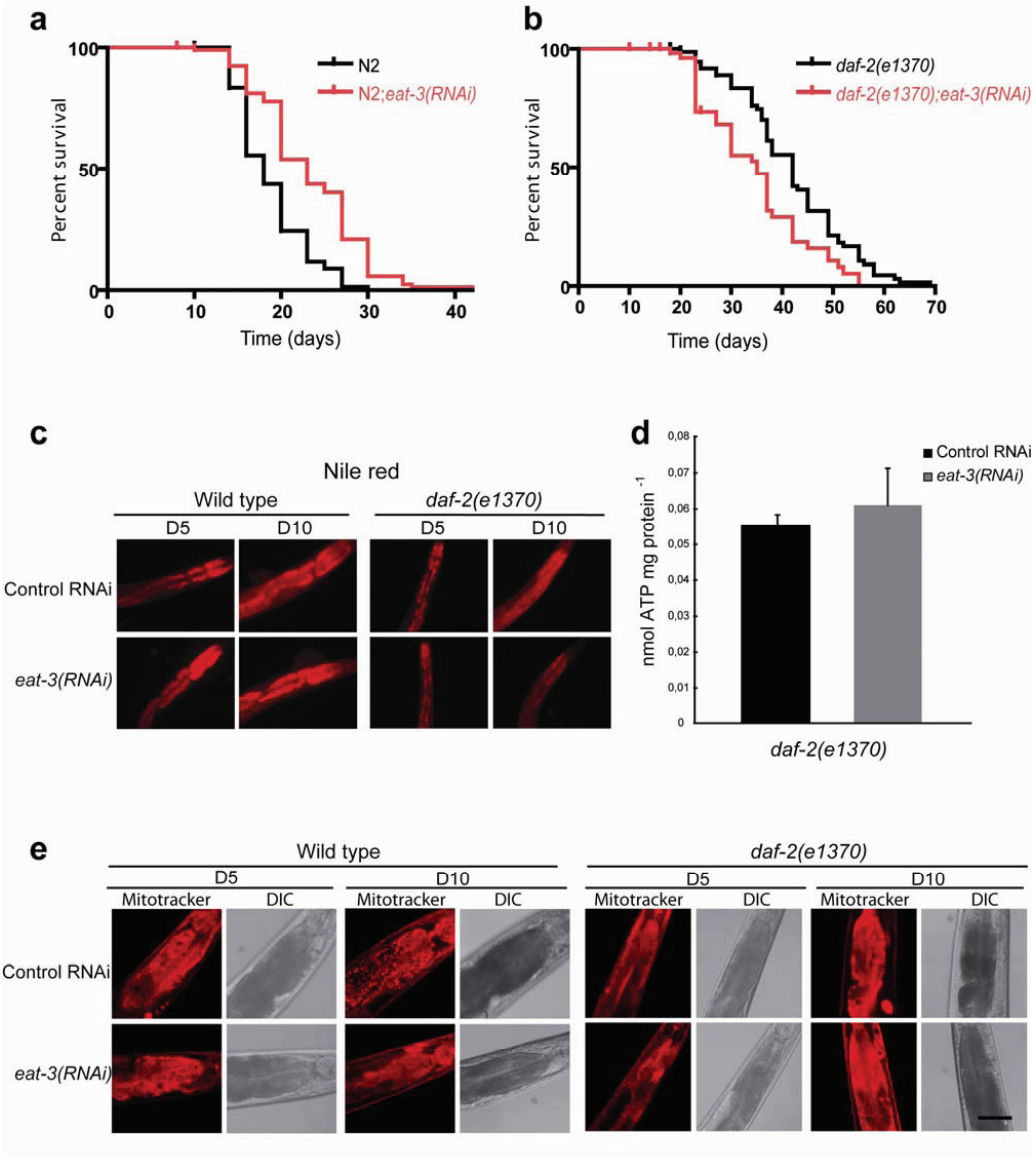

Figure S14 | Effects of depletion of the *C. elegans* Opa1 homologue EAT-3 on lifespan and metabolism. a, Survival curve of wild type animals subjected to *eat-3* RNAi. **b,** Survival curve of *daf-2(e1370)* mutant animals subjected to *eat-3* RNAi. The percentage of animals remaining alive is plotted against animal age. Lifespan values are given in Supplementary Table 1. **c,** Nile red staining of intestinal lipid depositions in wild type animals and *daf-2* mutants after RNAi knock-down of *eat-3*. **d,** Effect of EAT-3 depletion on the ATP content of *daf-2(e1370)* mutants. 10-day old adults were measured (error bars denote standard deviation). **e,** Mitotracker Deep Red 633 staining of intestinal mitochondria in wild type animals and dauer-defective *daf-2(e1370)* mutants subjected to *eat-3* RNAi. Images were acquired under the same exposure, using a 40x objective lens, at days 5 and 10 of adulthood (D5 and D10 respectively; see Methods; the anterior part of the intestine is shown, the head is located at the top; bar: 50 µm).

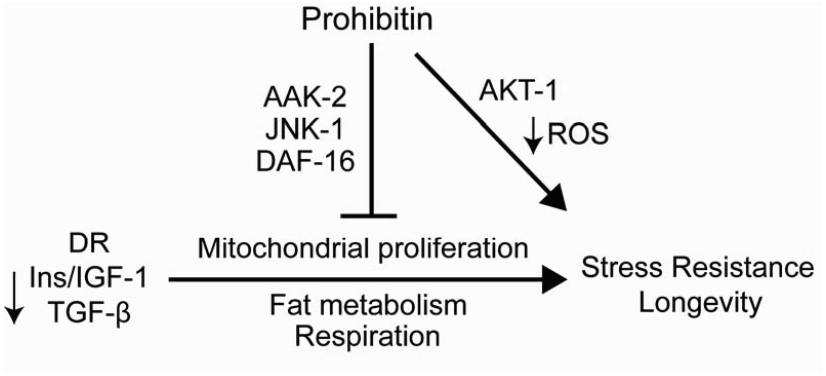

Figure S15 | Suggested model describing the opposite effects of prohibitin depletion on ageing. Under normal conditions prohibitin promotes survival by moderating mitochondrial function and ROS levels. Prohibitin depletion results in mitochondrial defects, increased ROS, and elicits a retrograde cellular response leading to mitochondria overproliferation and altered fat metabolism. Under reduced diapause signalling or stress where stress kinases and DAF-16/FOXO are activated, mitochondrial overproliferation is inhibited, promoting longevity (DR: dietary restriction, Ins: insulin).

Supplementary References

1. Artal-Sanz, M. *et al.*, The mitochondrial prohibitin complex is essential for embryonic viability and germline function in *Caenorhabditis elegans*. *J Biol Chem* 278 (34), 32091-32099 (2003).

2. Lin, K., Hsin, H., Libina, N., & Kenyon, C., Regulation of the *Caenorhabditis elegans* longevity protein DAF-16 by insulin/IGF-1 and germline signaling. *Nat Genet* 28 (2), 139-145 (2001).